LOW AND HIGH DENSITY OPERATION OF ALCATOR

G.J. Boxman°, B. Coppi*, L.C.J.M. de Kock°, B.J.H. Meddens°, A.A.M. Oomens°, L.Th.M. Ornstein°, D.S. Pappas*, R.R. Parker*, L. Pieroni†, S.E. Segre†, F.C. Schüller°, and R.J. Taylor*.

*Massachusetts Institute of Technology, Cambridge, Massachusetts, U.S.A.
°Association Euratom-FOM, Rijnhuizen, Jutphaas, The Netherlands
†Association Euratom-CNEN, Frascati, Italy.

Abstract: Two main plasma regimes are identified in Alcator, depending on the value of the streaming parameter, $\xi \equiv \langle u_{\parallel}/v_{the} \rangle$, where $u_{\parallel}$ and v_{the} are the electron drift and thermal velocities. For high $\xi (\gtrsim 0.4$ in $H_2)$ two-component electron distribution functions are obtained, rf emission at frequencies greater than and equal to the ion plasma frequency, and strong ion heating up to temperatures of 1 keV occurs. For low values of ξ (generally obtained by pulsed gas injection), the distribution function is Maxwellian; nearly classical resistivity and rates of bremsstrahlung emission are observed. The energy replacement time τ_E is found to increase roughly in proportion to the density. In the extremes of the two regimes $T_i \approx T_e$. Preliminary results of ion heating by rf injection near the lower hybrid frequency are reported.

Introduction: In this paper, we report on results obtained in Alcator[1], a tokamak device with major radius R = 54 cm, limiter radius a = 9.5 cm, and maximum toroidal field of 100 kG. The results reported here were obtained with toroidal fields in the range of 35 kG to 55 kG, with the bulk of the measurements taken at 40 kG. The corresponding plasma current range was 50 to 150 kA, with discharge duration from 70 to 400 msec. The base pressure was between 3×10^{-9} and 1×10^{-8} Torr. Vigorous discharge cleaning, accomplished by audio-frequency excitation of the ohmic system, preceded each run. The majority of the measurements were performed in hydrogen or deuterium. Additional measurements were performed in He and other gases or with a controlled dose of contaminants. Normal filling pressure was about 1×10^{-4} Torr; initial plasma density corresponds closely to this pressure. For clean machine conditions, the density always decreases with time, with the predominant decrease occurring in the first 5 msec of the discharge. In order to vary the plasma density, and therefore the electron flow velocity, additional gas is injected after toroidal equilibrium is established. In this way plasmas with average densities in the range of 5×10^{12} cm^{-3} to 2×10^{14} cm^{-3} have been investigated.

Proceed. 7th EPS (Lausanne) 1975 Vol. II

Two main regimes of operation are encountered by varying the value of the streaming parameter, $\xi \equiv \langle u_{\parallel}/v_{the} \rangle$ where $u_{\parallel}$ (v_{the}) is the local flow (thermal) velocity of the electrons; the average is over the minor toroidal cross section. In one, the classical or "Coulomb" regime which occurs for relatively high density and low values of ξ, the electron distribution function is nearly Maxwellian as measured by both laser and soft x-ray techniques. In the other, the anomalous or "slide-away" regime, characterized by relatively low density and high values of ξ, the electron distribution function inferred from these measurements is not Maxwellian. This regime is also characterized by strong heating of ions (up to $T_i \sim 1.2$ keV) accompanied by emission of rf radiation near ω_{pi}, lack of hard x-ray production (< 1 mR per shot near limiter), extremely low level of MHD instability and long stable discharges (up to 400 msec has been obtained). We believe that this is a new regime of tokamak operation.

Resistivity measurements: Examples of spectra obtained from pulse-height analysis of bremsstrahlung in the range 1-10 keV are shown in Fig. 1. We find the presence of an energetic tail in the slide-away regime, whereas we obtain a Maxwellian spectrum in the case of the Coulomb regime. An indication of similar effects is also obtained using laser scattering, and the results are documented elsewhere[2,3]. In the Coulomb regime, the peak temperature $T_e(0)$ determined from the soft x-ray measurement is systematically about 20% higher than that found from the laser, which may reflect a difference between transverse and longitudinal temperature. In the following we use the laser (transverse) temperature for evaluation of the classical resistivity.

We define

$$\xi \equiv \left\langle \frac{u_{\parallel}}{v_{the}} \right\rangle = \frac{2}{a_c^2} \int_0^{a_c} dr\, r \left[\frac{J_{\parallel}(r)}{en(r)}\right] \left[\frac{2T_e(r)}{m_e}\right]^{-\frac{1}{2}} \qquad (1)$$

where $J_{\parallel}(r)$, $n(r)$, and $T_e(r)$ are the current density, particle density, and electron temperature, and a_c is the effective radius of the current channel. We evaluate Eq. (1) by using the following radial profiles $T_e = T_e(0) \times \left[1 - (r/a_c)^{3/2}\right]$, $n = n(0)\left[1 - (r/a)^2\right]$ and $J_{\parallel}(r) \propto T_e^{3/2}(r)$ with $a_c = 8$ cm. These profiles are consistent with measurements made by the laser at 4 cm off centre. Using these profiles, we evaluate $\langle \eta/\eta_{cl} \rangle$, where $\eta = E_{\parallel}/J_{\parallel}$, η_{cl} is the Spitzer-Härm resistivity for hydrogenic plasma and $E_{\parallel}$ is the electric field (assumed to be constant over the cross section). In terms of the peak electron temperature $\hat{T}_{eo}$ (in units of keV)

$$\left\langle \frac{\eta}{\eta_{cl}} \right\rangle = 2.98 \frac{V}{\hat{I}} \hat{T}_{eo}^{3/2} S \,, \qquad (2)$$

where V is the loop voltage, $\hat{I}$ is the loop current in units of 100 kA, and S is a profile shape factor given by

$$S = \frac{2}{a_1^2} \int_0^{a_1} dr\, r \left[\frac{T_e(r)}{T_{eo}}\right]^{3/2} . \qquad (3)$$

(a_1 is the limiter radius).

Typical values of S found for other tokamaks range between 0.2 and 0.4. For the temperature profile used her S=0.23. Hence, the uncertainty in our temperature profile could lead to an underestimate of $\langle \eta/\eta_{cl} \rangle$ by a factor of 2.

Results for a variety of plasma densities, currents and filling gases are shown in Fig. 2. For each gas, a cross-hatched region is indicated which marks the transition region between Maxwellian and non-Maxwellian spectra. The data obtained for He was obtained by pulsed-gas injection into an initially hydrogenic discharge, with density about 5×10^{12} cm^{-3}. Since the density for the points obtained in Fig. 2c is greater than 2.5×10^{13} cm^{-3}, we believe that the majority of ions in these discharges are helium. We call attention to the fact that $\langle \eta/\eta_{cl} \rangle$ is never significantly greater than unity in H_2 and D_2, and approaches the classical value of 1.8 in He. There is also a systematic decrease in $\langle \eta/\eta_{cl} \rangle$ for $\xi > \xi_c$ for all gases.

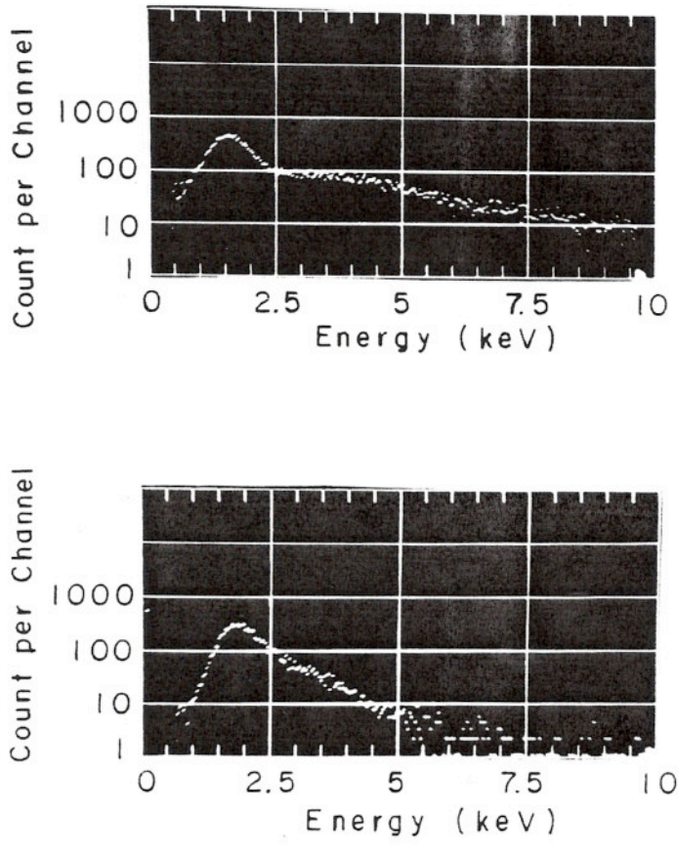

Fig. 1. Soft x-ray spectra obtained in slide-away (top) and Coulomb (bottom) regime.

We also report experiments concerned with effects of impurities on the resistivity measurements. Beginning with a well-conditioned machine, O_2 was injected into a hydrogenic discharge, and the partial pressure of O_2 was varied between 1 and 30×10^{-6} T. As a result, $\langle \eta/\eta_{cl} \rangle$ increased to about 2 and the electron temperature increased from 0.7 keV to 1 keV. The results

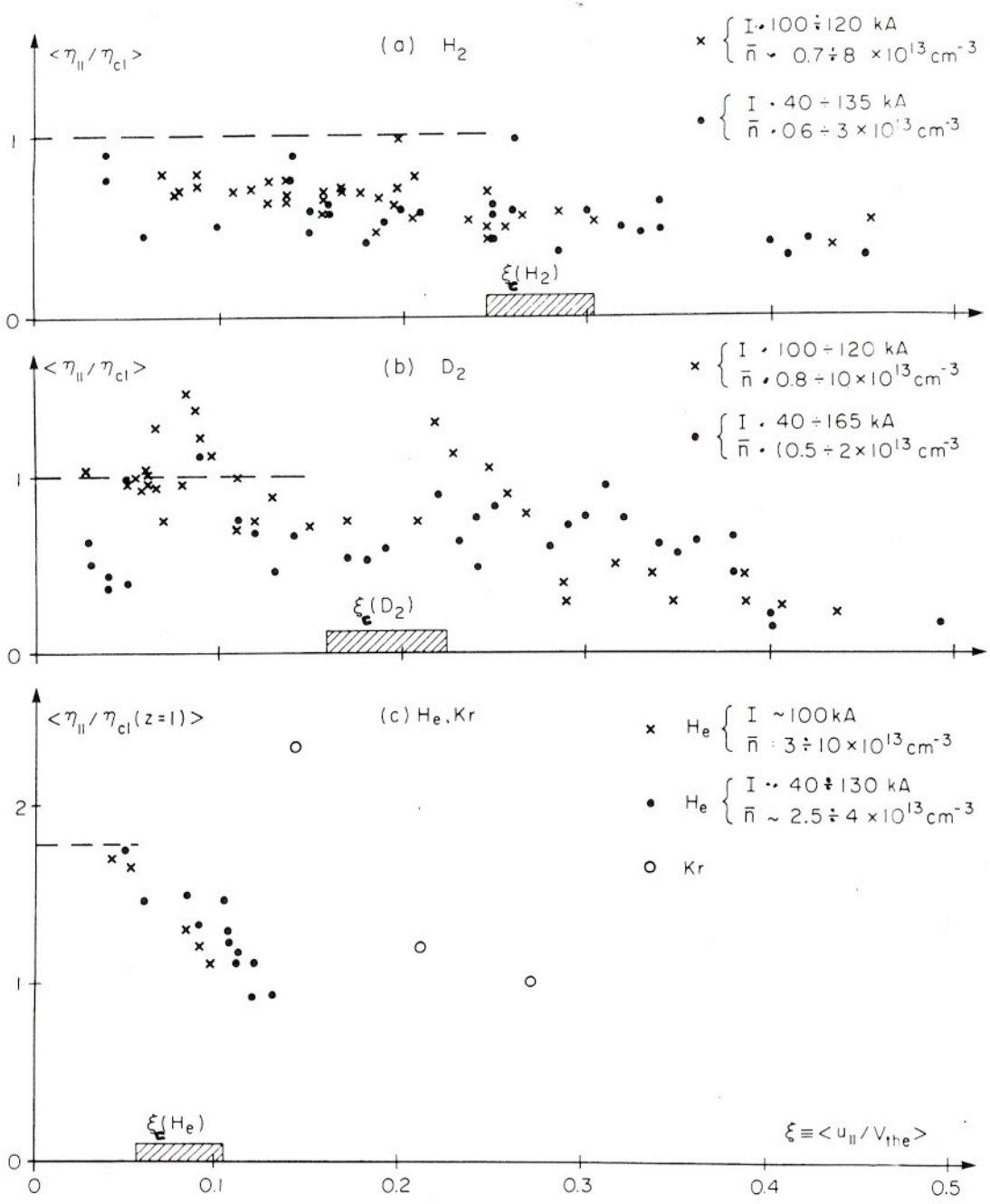

Fig. 2. Resistivity measurements in H_2 (a), D_2 (b), and He (c) as a function of the streaming parameter ξ.

are summarized in shots numbered 1-15 shown in Fig. 3. Then, normal tokamak operation ceased and the machine was discharge-cleaned in O_2 for about 30 min. Immediately, upon recommencing tokamak operation, $\langle \eta/\eta_{cl} \rangle$ increased to values of 3-5 and the electron temperature nearly doubled, as shown in shots 20-30 in Fig. 3. In addition to having higher voltage "anomaly" and electron temperature, these discharges differed in having an increasing rather than

the usual decreasing density with time, a much higher level of hard x-ray activity (100 mR/shot) and strong MHD instabilities[4]. Discharge cleaning in H_2 tended to reverse the process, but the normal duration of about 1 hr was not sufficient to reproduce the normal behaviour. Similar results were obtained by using N_2 rather than O_2 as the contaminating gas. We also note that values of ξ, obtainable for the contaminated machine, were generally in the range of 0.05-0.1. These results which show $\langle \eta/\eta_{cl} \rangle$ increasing to levels more typical of conventional tokamak operation give support to the credibility to results obtained under clean conditions.

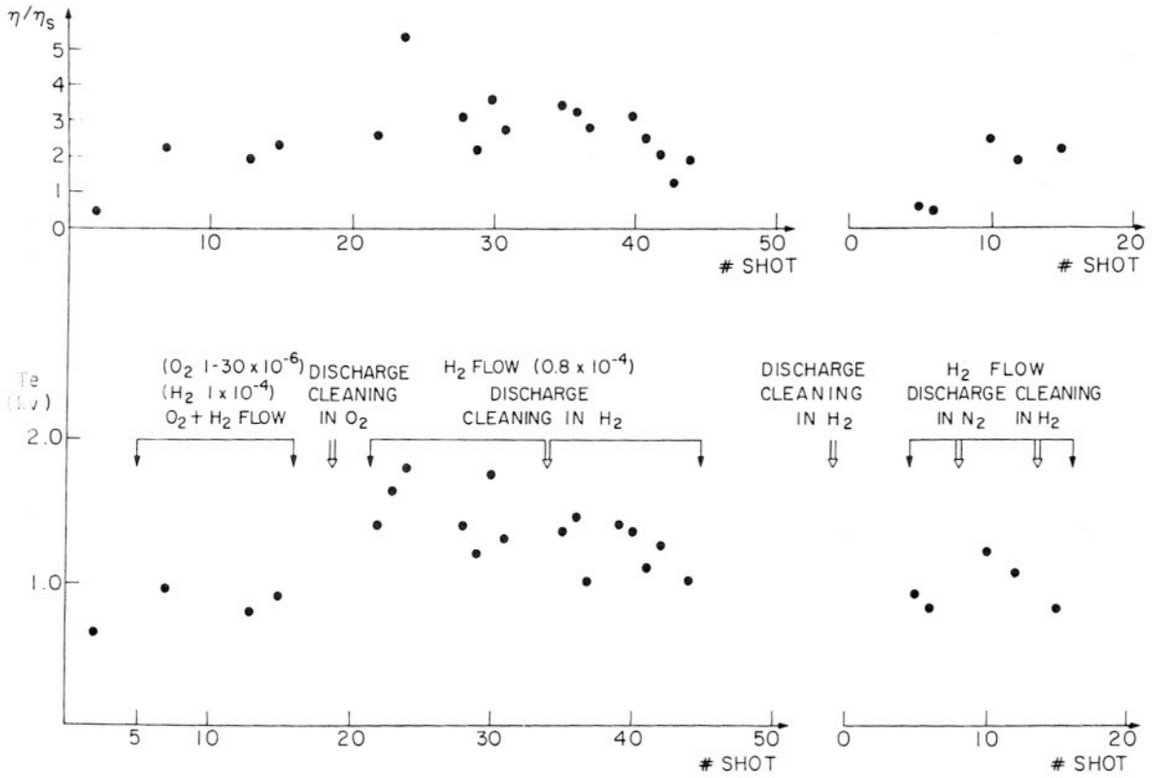

Fig. 3. Resistivity and temperature measurements in clean and contaminated conditions.

Below we will use a parameter α defined as $\alpha \equiv \langle \xi \rangle \langle \eta/\eta_{cl} \rangle$. In contaminated discharges the value of $\langle \eta/\eta_{cl} \rangle$ is increased, so that a higher value of α can be taken as an indication for a higher contamination level at the same value of ξ in different discharges.

Slide-away regime: Since plasmas with high ξ are known to be unstable in linear geometry (for example to ion-acoustic modes in the case $T_e > T_i$) we have been led to search for evidence of similar instabilities in the Alcator device. Additional motivation for this work was provided by the observation of high ion temperatures ($T_i \approx T_e \approx 1$ keV) even though the electron-ion equi-

libration time is much longer than the ion energy containment time. Here, we report the discovery of a band of strong rf emission in the vicinity of the ion plasma frequency ω_{pi}, extending from ω_{pi} to 5-10 ω_{pi}. The higher frequencies tend to occur first in time and correlate with the onset of hard x-ray emission (total dose $\sim$ 1 mR) and intense synchrotron radiation. The emission in the vicinity of ω_{pi} always occurs a few milliseconds later and correlates with the appearance of energetic ions (See Fig. 4). Thus, we identify the ω_{pi} radiation as being connected with the anomalous ion heating.

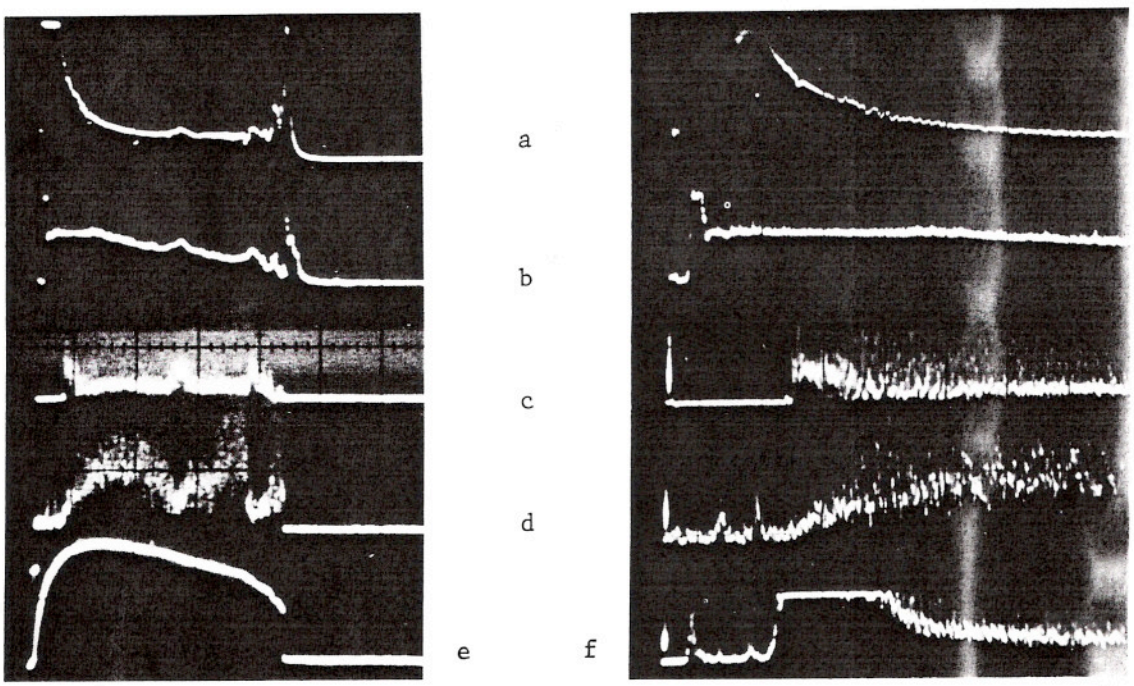

1. 2.

Fig. 4. Example of slide-away phenomena
a. loop voltage 1 V/div; b. electron density 1.2×10^{13} cm^{-3}/div; c. total rf-emission (arbitrary units); d. charge exchange neutrals: energy $\sim$ 2.5 keV; e. discharge current 65 kA/div; f. x-ray emission energy > 200 keV.
Sweep speed: 1. 50 msec/div; 2. 10 msec/div.

Measurements of the emission spectrum were taken with a small molybdenum-tipped probe, 0.6 mm in diameter. The probe is movable and can be positioned at any point within the 2.5 cm shadow of the limiter. Two spectrum analyzers were used to obtain the spectra in the ranges 300-2000 MHz and 1-20 GHz. The spectra were recorded by either repeated, fast (10 msec) sweeping of the analyzer, or by shot-to-shot scanning of the passband frequency.

In Fig. 5, we present the spectra obtained at three moments in time during the discharge. A strong peak at the lower end of the spectrum is found at frequencies corresponding to $f_{pi} = 210\sqrt{n_e/A}$, where A is the ion mass number. This dependence is displayed in Fig. 6, where we have plotted the density calculated by assuming the peak of the spectrum to correspond with f_{pi} vs

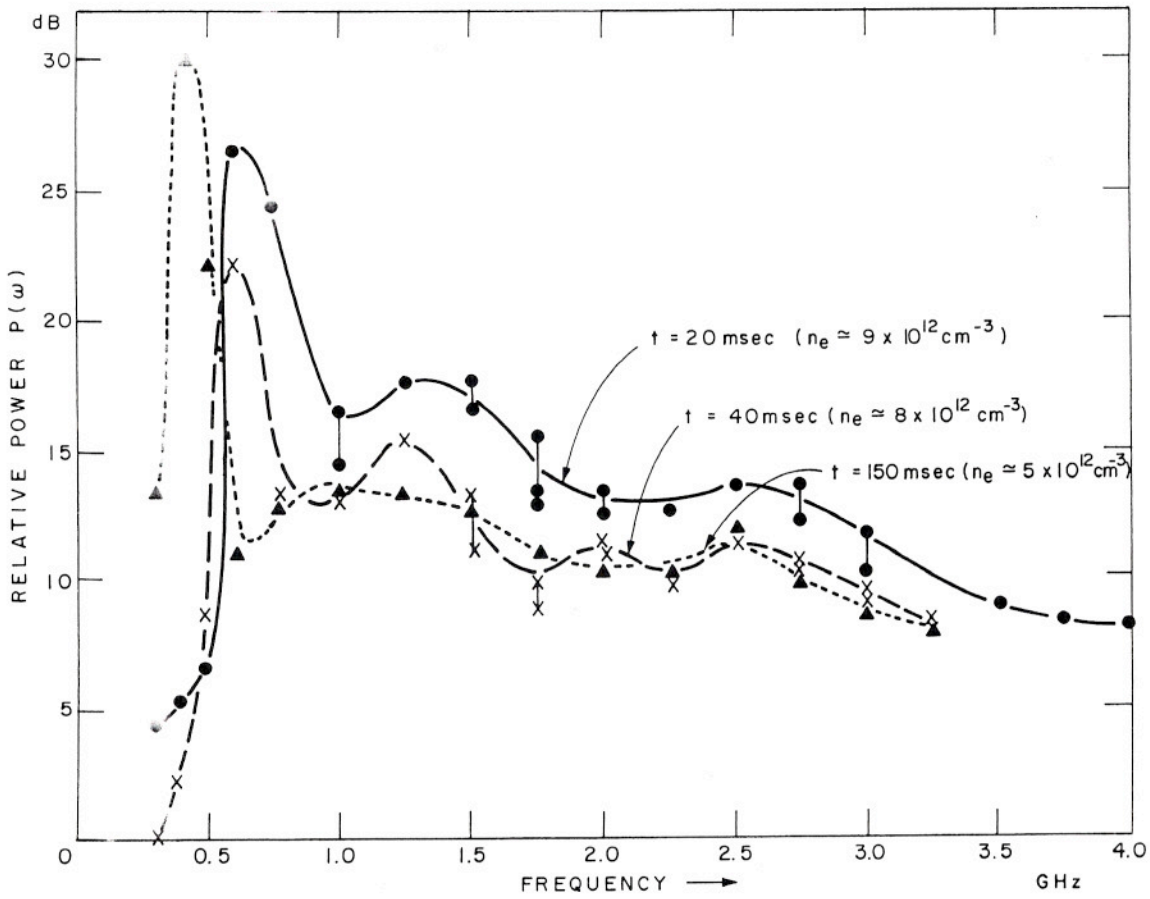

Fig. 5. Spectral emission from a slide-away discharge in hydrogen; shot-to-shot measurements were taken at B_ϕ = 40 kG, I = 100 kA.

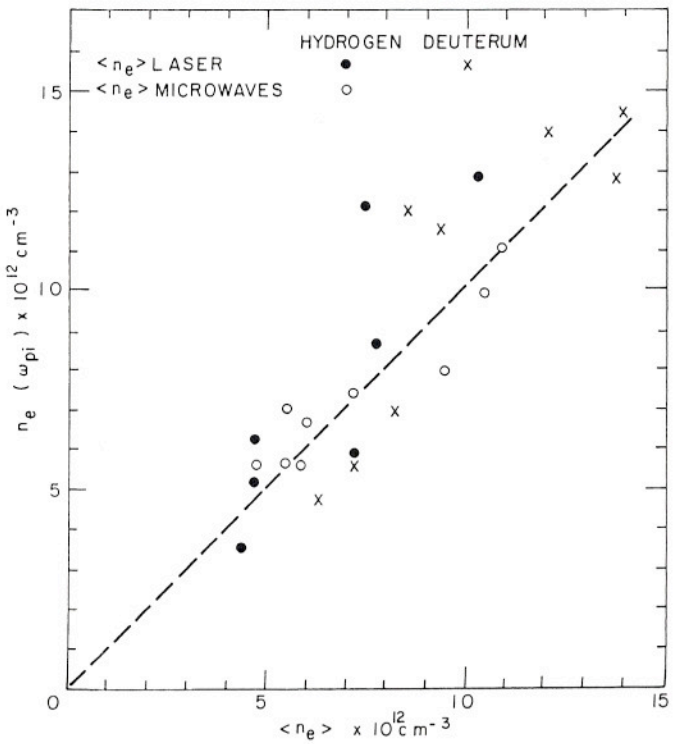

Fig. 6. The electron density $n_e(\omega_{pi})$ calculated when the measured peak frequency is interpreted as ω_{pi} vs the measured electron density $\langle n_e \rangle$.

the actual average density as measured by either 4 mm or 2 mm interferometers or by calibrated Thomson scattering. A 30 dB drop in the intensity is observed just below f_{pi}, and when the average density decreases during a discharge pulse, this cut-off moves

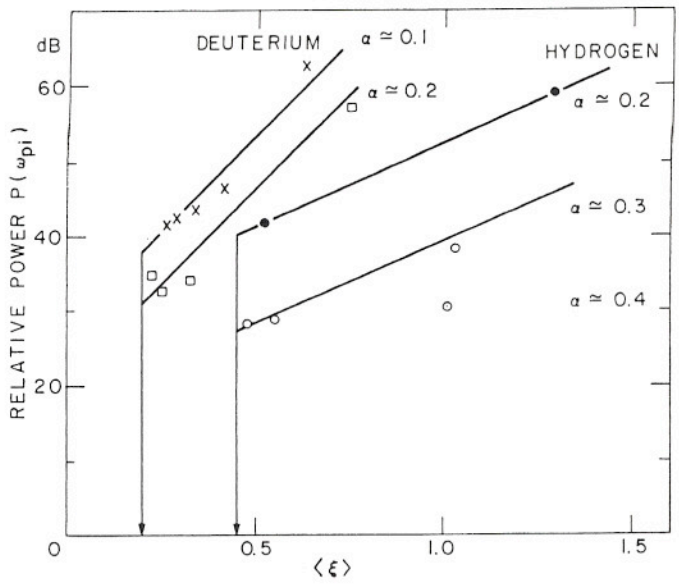

Fig. 7. Relative power level $P(\omega_{pi})$ of the radiation emitted at ω_{pi}.

accordingly. The spectrum extends to several GHz where the emission level becomes comparable to the sensitivity of the analyzer (∿ 45 dB). The relative power $P(\omega_{pi})$ of the emitted radiation at f_{pi} as a function of ξ is found to have a distinct threshold at values of 0.45 for hydrogen and 0.2 for deuterium discharges as shown in Fig. 7. There are also indications that the presence of impurities leads to a decrease of the emitted power. Discharges with higher impurity content (α = 0.3 to 0.4) have $P(\omega_{pi})$ decreases by 15 to 20 dB.

The fact that the emission is cut off below ω_{pi} tends to rule out turbulence associated with classical current-driven ion-acoustic waves. In this regime of operation $\omega_{pe}^2 >> \omega_{ce}^2$ and the lower hybrid resonance frequency $\omega_{LH} \approx \omega_{pi}$. This suggests the excitation of lower hybrid modes which propagate for $\omega > \omega_{pi}$, whose mechanism has been investigated[5].

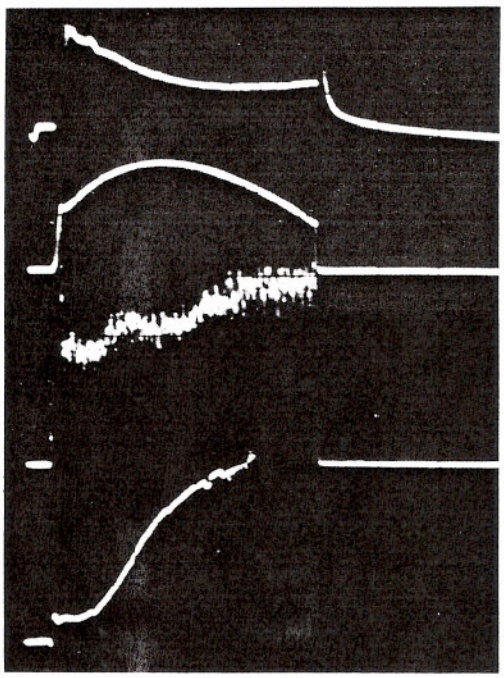

Sweep speed: 20 msec/div.

Coulomb regime: After formation of a discharge at normal filling pressure of 1×10^{-4} T, gas is injected by means of a pulsed gas valve. In this way, discharges with $\langle n_e \rangle$ up to 2×10^{14} cm^{-3} have been studied. Typical traces of voltage, current, and density for this mode of operation are shown in Fig. 8. In this mode, the electron and ion distribution functions are nearly

Fig. 8. Example of a discharge in the Coulomb regime: a loop voltage 2 V/div; b. discharge current 65 kA/div; c. O^{VI} emission at λ = 1032 Å, 6.8×10^{15} photons/sec/cm^2.sterad/div; d. electron density 4.6×10^{13} cm^3/div.

Maxwellian (c.f. Fig. 1.b), and the resistivity appears to be close to classical as evidenced by data presented in Fig. 2 for $\xi << \xi_c$. Both soft x-ray and visible bremsstrahlung measurements show that the effective Z (defined here as the ratio of measured to computed free-free hydrogenic bremsstrahlung decreases from 5-10 at low density ($\sim 1\times10^{13}$ cm^{-3}) to near unity at high density (1×10^{14} cm^{-3}). This implies that the relative impurity concentration in the centre of the plasma decreases as the density is increased, a conclusion which is also supported by the density dependence of the UV-lines of light impurities, for example, O^{VI} as shown in Fig. 8.

Poloidal beta $\beta_\theta \equiv \langle nk(T_e+T_i)\rangle / B_0^2(a_1)/2\mu_o$ and gross energy replacement time $\tau_E \equiv \frac{3}{2}\langle nk(T_e+T_i)\rangle$Volume/I.V. have been measured (see Fig.9). Here the profiles quoted above are used. The data points represent τ_E, neglecting the ion energy content, and the dashed line indicates the effect of including the ions. The energy replacement time is roughly proportional to n_e and has weak (if any) dependence on I and B_ϕ. The poloidal beta, consistent with the measurement of τ_E, scales as $\beta_\theta \propto n_e/I^p$, where $p \approx 1$. We also find the maximum density is proportional to the maximum value of I, which suggests a limiting value of β_θ.

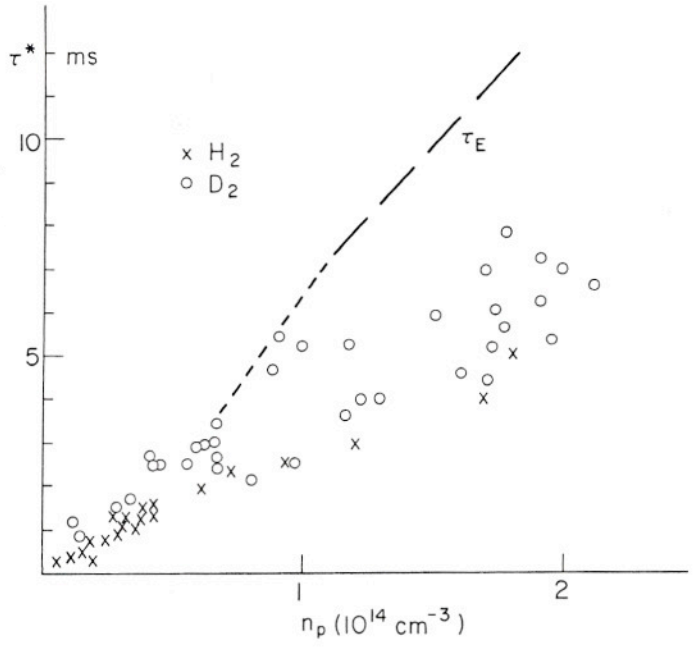

Fig. 9. Energy replacement time vs density.

R.F. heating: Ion heating by rf injection near lower hybrid frequency ω_{LH} has also been studied[6]. A pulse of rf power, frequency 2.45 GHz, peak power 70 kW and width variable up to 100 msec have been applied by means of an S-band waveguide flush-mounted in the vacuum chamber wall and oriented so that $\vec{E} \parallel \vec{B}$. The total absorption efficiency is high with 70-80% of the forward power absorbed. No deleterious effects (such as density rise or impurity increase) on the discharge are found. Typical ion temperature rise is on the order of 100 eV (see Fig. 10). Strong tail-heating is also observed; the effect is nonlinear in the applied power. For ion heating to occur, it is not necessary to satisfy $\omega = \omega_{LH}$ anywhere in the plasma.

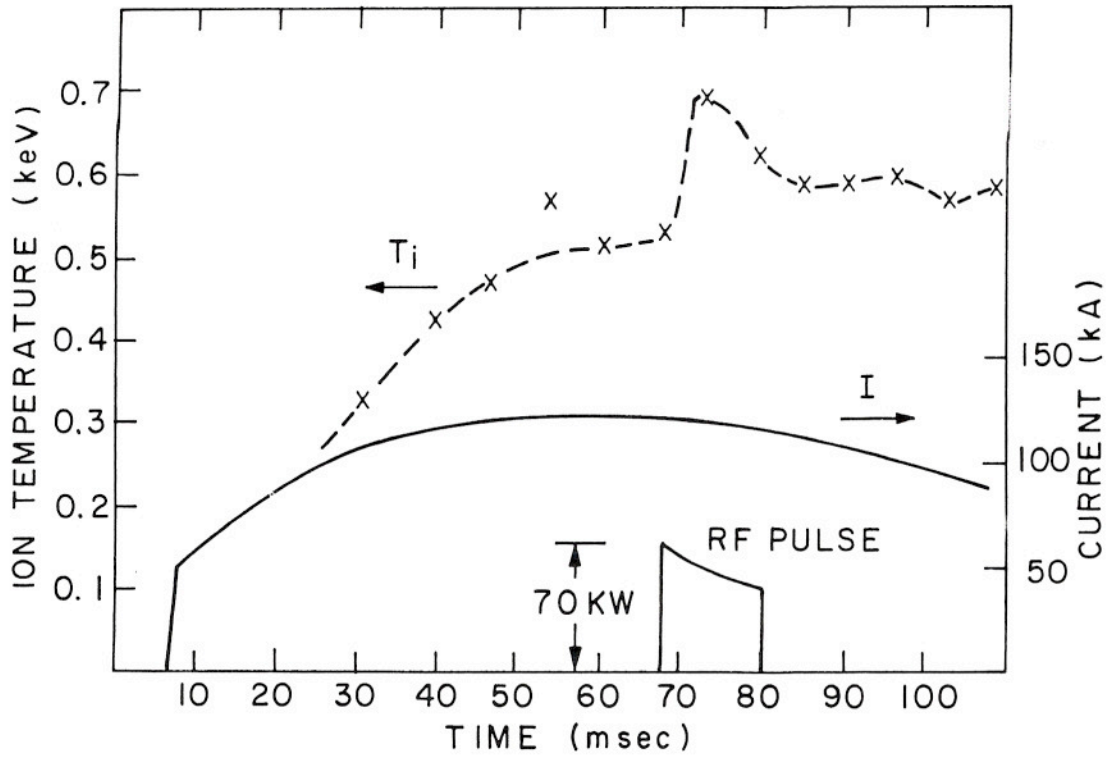

Fig. 10. Development of the ion temperature with rf heating applied.

Acknowledgements

Supported in part by the U.S. Energy Research and Development Administration, Contract E(11-1)3070, the Association Euratom-FOM, Rijnhuizen, Jutphaas, The Netherlands and the Association Euratom-CNEN, Frascati, Italy.

It is a pleasure to acknowledge the contributions of the staff and the use of the facilities of the Francis Bitter National Magnet Laboratory supported by the National Science Foundation.

References

[1] Ascoli-Bartoli, U. et al., Proc. Fifth Int. Conf. on Plasma Phys. and Contr. Nucl. Fusion Research, Tokyo, 1974, I, 191, P. IAEA-CN-33/A 8-4.

[2] Pieroni, L. and Segre, S.E., Phys. Rev. Letters 34 (1975) 928.

[3] Segre, S.E. and Pieroni, L., Phys. Letters 51A (1975) 25.

[4] De Kock, L.C.J.M., et al., Rijnhuizen Report 74-86 (1974).

[5] Coppi, B., et al., M.I.T.(Cambridge, Mass.) Report PRR 758 (1975) (Submitted to Nuclear Fusion).

[6] Parker, R.R., R.L.E.-M.I.T. (Cambridge, Mass.) Quarterly Progress Report 102 (July 1971).